Development of Hybrid Titania/Polybenzoxazine Composite for Enhance Thermo-Mechanical, Flame Retardancy and Dielectric Properties

shakilaparveen asrafali (shakilaasraf@gmail.com)
Yeungnam University

Research Article

Keywords: polybenzoxazines, benzonitrile, TiO2 fillers, composites, superhydrophobic

Posted Date: March 18th, 2022

DOI: https://doi.org/10.21203/rs.3.rs-1434024/v1

Abstract

Polybenzoxazines (Pbzs) are recently developed class of thermosetting polymeric materials possessing low surface free energy with non-fluorine or non-silicon content. In the present study, a new type of Pbz-BN/TiO_2 composites were fabricated using benzoxazine monomer [bis(6-phenyl diazenyl-3-phenoxy-3,4-dihydro-2H-1,3-benzoxazinyl) benzonitrile] and inorganic TiO_2 fillers by a simple and inexpensive process. Thermal curing method was found to be effective for preparing superhydrophobic surfaces combining low surface energy and surface roughness. The presence of benzonitrile group in the benzoxazine monomer paves way for accelerating the curing of the benzoxazine monomer as shown by the DSC analysis. The as-prepared Pbz/TiO_2 surfaces containing 5 wt% of TiO_2 generated a superhydrophobic surface exhibiting static water contact angle (SWCA) of 146°. In addition to it, the effect of inorganic fillers on the thermal, mechanical and dielectric properties of the Pbz/TiO_2 composites was investigated in detail.

Introduction

Polybenzoxazine (Pbz), as a new class of thermosetting phenolic resins has been developed to overcome the shortcomings of traditional phenolic resin, while keeping the advantages of cost effectiveness, heat resistance and flame retardancy. Benzoxazine based thermosets exhibit high glass transition temperature and high modulus even though they have relatively low crosslink densities owing to strong hydrogen bonding restricting segmental mobility and impeding network formation[1–5]. In spite of these, Pbz is considered as a new class of low surface energy materials and exhibits a large number of interesting properties, such as near zero shrinkage during curing, high carbon content, low water absorption, high thermal stability, excellent electrical properties etc. Low surface energy is important for many practical applications in coatings, self-cleaning materials and biomaterials[6–9].

Several studies have been conducted to improve the mechanical properties of polymers, such as strength, toughness and elastic modulus, among which the combination of nanoparticles (NPs) is one of the most current research topics. Since NPs are usually aggregated due to the strong van der Waals force, it is very difficult to achieve mono-dispersity in a resin matrix at the nanoscale. Agglomerated fillers not only suffers the mechanical properties of the cured matrix, but also act as initiation points of cracks and fractures, which even deteriorate the mechanical properties. In other words, one of the critical issues is to achieve a non-aggregated dispersion of the integrated NPs to impart the polymer matrix its remarkable mechanical, electrical and thermal properties. Their dispersion characteristics and interfacial adhesion can be improved by modifying the NP surface with suitable dispersants or polymer coating[9–16].

Modification of nano fillers with functional benzoxazine monomer (Bzo-BN) has proven to be a promising approach to prepare nanocomposites by exploiting high flexibility of benzoxazine molecular design by synthesizing titania/polybenzoxazine nanocomposites via thermal curing process. Transparent hybrid films were obtained, suggesting dispersion of nano sized titania particles in a polybenzoxazine matrix.

Novel polymer composite with nano-TiO_2 content reinforced with polybenzoxazine were prepared. The adhesion between nano-TiO_2 and Pbz-BN was found to be strong, and the distribution of nano fillers was relatively uniform; a novel benzoxazine with benzonitrile functionalization (Bzo-BN) was prepared and blended with TiO_2 (with different ratios) leading to the formation of highly dispersible organic/inorganic polybenzoxazine/TiO_2 hybrid composites[17–24].

The effect of dispersion of different wt% of TiO_2 particles in benzoxazine was investigated by analyzing their polymer properties, viz., mechanical, thermal, water resistance and dielectric properties. TiO_2 was used in this work as it has a linear coefficient of thermal expansion closer to that of the polymer matrix and other excellent properties, such as high strength and surface toughness and excellent wear resistance. Although several studies on the effect of various dispersants on the mechanical behavior of polybenzoxazine nanocomposites have been reported previously, no studies based on benzoxazine/TiO_2 matrices have been reported. Therefore, our preparation and evaluation procedure provides a good way to facilitate the dispersion of inorganic NPs with benzoxazine dispersants and to further improve the mechanical properties of benzoxazine/TiO_2 composites.

Experimental

Materials and methods

The materials, instrumentation methods, synthesis of precursors, i.e., 4-(phenyl diazenyl) phenol [PAP] and 4,4’ bis(4-aminophenoxy) benzonitrile [APBN] and structure analysis of these precursors are given in the ESI.

Synthesis of bis(6-phenyl diazenyl-3-phenoxy-3,4-dihydro-2H-1,3-benzoxazinyl) benzonitrile [Bzo-BN]

To start with, paraformaldehyde (1.8 g, 0.06 mol) was dissolved in DMSO (50 mL) at 100 ℃. To the dissolved solution, the synthesized diamine (APBN, 3.2 g, 0.01 mol) and the phenol (PAP, 3.9 g, 0.02 mol) were added in parts and the reaction mixture was further increased to 130 ℃. After completion of reaction, the reaction mixture was allowed to reach room temperature and the product precipitated in 1N NaOH solution. The collected precipitate was water washed to remove any un-reactants, filtered and dried at 60 ℃ to afford brown powder of Bzo-BN monomer [Scheme 1]. Yield: 82%

FT-IR (KBr, cm^{-1}): 936 (stretching vibrations of the oxazine ring), 1256 & 1045 (asymmetric and symmetric stretching vibrations of C-O-C), 1177 (stretching of C-N-C), 1340 (CH_2 wagging), 2246 (-CN stretching vibrations), 1445 (trans N=N stretching vibrations); ^{1}H-NMR ($CDCl_3$, ppm): 5.4 (s, H_a, 4H), 4.6 (s, H_b, 4H) and 6.5–8.0 (m, aromatic protons); ^{13}C-NMR $CDCl_3$, ppm): 79 (O-CH_2-N), 50 (Ar-CH_2-N), 115 (-CN), 94 (Ar (C)-CN) and 110–155 (aromatic carbons).

Preparation of Pbz-BN/TiO_2 composites

Pbz-BN/TiO_2 composites with varying ratios of TiO_2 were prepared. Briefly, the synthesized Bzo monomer and TiO_2 (1 wt% of Bzo-BN) was mixed with THF and stirred well to form a homogeneous solution. This solution was then poured onto petridish, pretreated with dichlorodimethyl silane (for easy release of the cured film) and then cured maintaining the temperature at 250 ℃ for 3h. The cured films were then taken out with care. Pbz/TiO_2 composite thus prepared was denoted as Pbz-BN/T1. Similarly, other ratios of Pbz/TiO_2 composites were denoted as Pbz-BN/T0; Pbz-BN/T3 and Pbz-BN/T5, respectively with varying the weight ratio of TiO_2.

Results And Discussions

Structural analysis of benzoxazine monomer [Bzo-BN]

The FT-IR spectra of the synthesized benzoxazine monomer [Bzo-BN] was shown in Figure 1. It can be seen from the figures that the benzoxazine ring is characterized by the absorption bands between 936 cm^{-1}, due to the stretching vibrations of the oxazine ring. Moreover, the benzoxazine ring also gave its characteristic absorption band at 1219 cm^{-1}, 1021 cm^{-1} due to the asymmetric and symmetric stretching vibrations of the C-O-C bond, stretching vibrations of the C-N-C bond respectively[25]. The nitrile (-CN) group show their characteristic absorption bands at 2246 cm^{-1}. Figure 2, illustrates the ^{1}H-NMR and ^{13}C-NMR spectra of the benzoxazine monomer Bzo-BN. The oxazine ring protons (H_a, O-CH_2-N and H_b, Ar-CH_2-N) show two singlets at 5.4 and 4.6 ppm, respectively[26-28]. The aromatic ring protons are located between 6.5 - 8.0 ppm. The ^{13}C-NMR spectrum shows the characteristic carbon resonances of Bzo-BN. The methylene carbons [O-CH_2-N (C_1) and Ar-CH_2-N (C_2)] of the oxazine ring resonate at 79 and 50 ppm, respectively. The carbon of the benzonitrile group (C_3) resonates at 115 ppm. And the aromatic carbon attached to the benzonitrile group (C4) resonates at 94 ppm[29]. All other aromatic carbons resonate between 110 - 155 ppm, respectively.

Polymerization behavior of hybrids

DSC of the hybrids was performed to study the polymerization behavior of benzoxazine monomer in presence of TiO_2 by monitoring the typical exothermic peak attributed to the ring opening polymerization of benzoxazine (Bzo-BN) and their hybrids (Bzo-BN/T0-T5). DSC showed that the neat benzoxazine monomer exhibits an exothermic curve with T_{onset} at 224 ℃, T_{max} at 243 ℃ and T_{final} at 256 ℃. In comparison, for the hybrids, the exothermic curve shows that T_{onset} slightly shifted to lower temperature (218 ℃) and T_{max} and T_{final} shifted to 251 and 262 ℃, respectively. This result indicates that the ring opening polymerization of benzoxazine monomer has been accelerated by the presence of nitrile group (act as a catalyst) and thus lowers its onset of curing temperature. The addition of TiO_2 particles into the Bzo monomer shifts the maximum and final curing temperature to higher value, which could be due to the trapped TiO_2 particles inside the monomer. Moreover, the ΔH value of Bzo-BN/TiO_2 hybrids decreases with increasing TiO_2 content. This is due to the fact that with increased TiO_2 content, the Bzo content in

the Bzo-BN/TiO_2 hybrid decreased obviously, thus reducing their enthalpy values. Similar exothermic curing behavior was observed for BA-a/inorganic nano fibers (30 wt%), where, the maximum curing temperature of neat BA-a (240 ℃) was shifted to 250 ℃ with incorporation of the inorganic materials[30,31].

Table 1 Data from DSC thermograms of Bzo-BN/TiO_2 hybrids

S.No.	Sample	TiO_2 ratio	T_{onset} (°C)	T_{max}(°C)	T_{final} (°C)
1	Bzo-BN/TiO_2	0	224	243	256
2		1	223	245	258
3		3	220	248	261
4		5	218	251	262

Morphology of PBz-BP/TiO_2 composites

Figure 4 shows the SEM micrographs of PBz-BN/TiO_2 composites. The smooth surface of pure polybenzoxazine is clearly visible from the figure. As the titanium content increases (from 1 to 5% by weight), the surface of the composites loses its smoothness and becomes rough. It also shows the formation of homogeneous hybrid material and fine dispersion of titanium particles. The small size of the titanium particles may be responsible for the transparency of the hybrid materials[32]. As the TiO_2 content increases to 5% loading, few voids or gaps appear on the surface of the composites. AFM images (Fig. 5) of polybenzoxazine and their composites show that the size of the nodules formed by the Pbz-TiO_2 particles is uniform and has a uniform distribution, as seen in the SEM images. The surface roughness of polybenzoxazine-silica hybrids was calculated from AFM measurements using the following equation[33],

$$R_t = R_p + R_v$$

Where R_t is the total roughness of the measured sample, R_p is the maximum peak height of the profile, and R_v is the maximum valley depth of the profile. The total roughness was found to be 8, 83, 109, and 128 nm for Pbz-BP:T0, Pbz-BP:T1, Pbz-BP:T3, and Pbz-BP:T5, respectively. The roughness value increases with increasing titanium content from 1 to 5 wt%, which is consistent with the AFM images.

Surface Properties of the polybenzoxazine-titania hybrids

As is known, superhydrophobic surfaces can be prepared by combining low surface area and free energy materials with rough structures. In this case, Pbzo-BN with a network of hydrogen bonds and nitrile

structures were used as a low surface area and free energy material[34]. The addition of TiO_2 NPs was able to form rough structures. Figure 6 shows the WCAs of neat polybenzoxazine and polybenzoxazine-titania hybrid [Pbz-BP:T1, Pbz-BP:T3 and Pbz-BP:T5] coatings with different mass ratios of TiO_2 NPs. The pure Pbz coating showed hydrophobicity with a WCA of 87°. With the increase of the additional amount of TiO_2 NPs, the hydrophobicity of the Pbz/TiO_2 also increased significantly with a linear increase in WCA from 87 to 146 °C. The hydrophobicity of polybenzoxazine was improved by incorporating TiO_2 nanoparticles even at low concentrations (e.g. 5 wt% TiO_2). The increased hydrophobicity of the [Pbz-BP:T5] hybrid is attributed to the air trapped in the voids of the rough surface and preventing water from entering the nanoparticles, leading to an increase in the contact angle with water[35].

Dynamic mechanical Properties of titanium-modified polybenzoxazine hybrids

The dynamic mechanical properties of the hybrid materials in comparison to neat polybenzoxazine were examined. Fig. 7 shows the storage modulus (E') and loss modulus (E") as a function of temperature. The storage modulus of the neat Pbz drops slowly up to 125 °C, after which there is a sharp drop with a glass transition temperature (T_g) of 147 °C obtained from the maximum of loss modulus. The storage moduli of the composites in the glassy state increase with the inclusion of titanium particles, and rise more on further increasing the content of titanium in the hybrids[36-38]. This behavior indicates that the dispersed titanium nanoparticles are effective to reinforce polybenzoxazine matrix. The drastic improvement of the storage modulus of polybenzoxazine by hybridization with small amount of titanium nanoparticles (5%) can be attributed to the reinforcing role of the titanium nanoparticles and the increase of the polymerization degree of polybenzoxazine via their nitrile group on the ring opening polymerization similar to the role of silica, clay and other inorganic nanomaterials on polybenzoxazines nanocomposites as previously reported[37,39]. Also, the hybrids show higher T_g than the neat resin. The T_g of pure polybenzoxazine was found to be 147 °C; but for the composites, the T_g increased with increasing nano filler content (T_g of Pbz-BP/T5 is 164 °C). The hard and rigid inorganic regions create an obstacle to the movements of random chain segments in the matrix. This restricted mobility of the segmental molecular chains results with an increased T_g values. A similar increase in T_g values is observed in PBA-a composites with other inorganic nanofibers, ranging between 185 and 193 °C[40-43].

Table 2 DMA data of Pbz-BN/TiO_2 composites

S.No.	Sample	TiO_2 ratio	DMA		
			Storage modulus	T_g (°C)	CLD *10^5 mol/m^3
1	PBz-BN/TiO_2	0	2.81	147	3.7
2		1	3.15	151	4.1
3		3	3.21	157	4.2
4		5	3.26	164	4.3

Cross-link density of Pbz/TiO_2 composites

The cross-link density (CLD), γ_c is the number of network chain molecules per unit volume of the cured polymer. The cross-linking density of highly cross-linked thermoset materials can be determined by modulus measurements using the modulus constitutive equation given below[44],

$\gamma_c = $ □'/3RT

Where,

□' = storage tensile modulus (from DMA)

T = temperature in K corresponding to the value of the storage modulus

R = gas constant

Table 2 shows the interconnect density of the Pbz/TiO_2 composites. The crosslinking density of the pure polymer, i.e. Pbz-BN/T0, was found to be 3.7*10^{-5} mol m^{-3}, while the crosslinking density of the composite, i.e. Pbz-BN/T5, was found to be 4.3*10^{-5} mol m^{-3}. It can be seen that the crosslinking density obviously increases with the increase in the nanoparticle content in the composites. The main reason is that the nanoparticles behave as natural cross-linkers by forming intermolecular hydrogen bonds between the hydroxyl groups of the nanoparticles and the -OH, -CN, of the polybenzoxazine(s), thus limiting their molecular motion[45,46].

Thermal stability of Pbz/TiO_2 composites

The thermal stability of the hybrids was studied by thermogravimetric analysis to investigate the effect of dispersed titanium particles on the thermal stability of the polybenzoxazine matrix. Figure 8 shows the TGA profiles under nitrogen atmosphere of pure Pbz and the composites containing various percentages of titanium. For pure Pbz, T_5 and T_{10} are 326 & 354 °C with a carbon yield of 42.6%. The incorporation of

titanium particles in the Pbz matrix led to an increase in thermal stability. For example, the carbon yield increased from 42.6 to46.4, 51.2 and 53.7% with the addition of 0, 1, 3 and 5 wt% titania, suggesting that the dispersed titanium particles in the matrix act as a thermal insulator to protect the Pbz matrix. Also, the composites also contain nitrile group, by which the thermal stability showed a greater improvement. This could be attributed to the maximized adhesion between the organic (Pbz) and inorganic (titanium) sites, which further protect the organic matrix with thermal insulation[47-49].

Table 3 TGA data of Pbz-BN/TiO_2 composites

S.No.	Sample	TiO_2 ratio	T_i (°C)	T_5 (°C)	T_{10} (°C)	CY	LOI
1	PBz-BN/TiO_2	0	286	326	354	42.6	34.5
2		1	296	351	374	46.4	36.1
3		3	308	364	386	51.2	38.0
4		5	313	378	403	53.7	39.0

Flame retardancy of Pbz/TiO_2 composites

The flammability resistance of pure Pbz and Pbz-TiO_2 composites is explained as a function of the limiting oxygen index (LOI) value. One way to calculate the LOI is by TGA analysis, knowing their corresponding carbon yield values. van Krevelen and Hofytzer used the equation[50] given below to calculate the LOI,

LOI=17.5+0.4*CY

Where,

LOI is the oxygen limit index,

CY is the carbon yield (from TGA data).

The value of LOI for the pure Pbz-BN polymer was 34.5. And their composites showed LOI values of 36.1, 38.0 and 39.0 for Pbz-BN/T1, Pbz-BN/T3 and Pbz-BN/T5, respectively (Table 3). It could be observed that the LOI value of polybenzoxazine and their composites were higher than the threshold value (26). This clearly indicates that the incorporation of TiO_2 nanoparticles in the Pbz system results in thermosets with good self-extinguishing and flame retardant properties.

Dielectric properties of Pbz/TiO_2 composites

Dielectric materials can be used to store electrical energy in the form of charge separation when the electron distributions around their constituent atoms or molecules are polarized by an external electric field. The dielectric constant is directly related to the polarizability of the material and is therefore highly dependent on its chemical structure. Figure 9 shows the values of the dielectric constant and the dielectric loss of Pbz/TiO_2 composites. The values of dielectric constant and dielectric loss were found to be in the range of 3.2 - 2.9 and 0.94 - 0.78, respectively for Pbz-BN/TiO_2 composites, respectively (Table 4). Composites differ from micro composites in three aspects: they contain small amounts of fillers, the filler particles have sizes in the order of nanometers, and the interface between the filler and the polymer is large. Nanoparticles reduce the movement of the polymer chain by physical bonding[51]. The mobility of the charge carriers, also decreased with particle loading, suggesting that the nanoparticles disperse the carriers by reducing their mobility, leading to a decrease in permeability with increasing frequency[52].

Table 4 Dielectric data of Pbz-BN/TiO_2 composites

S.No.	Sample	TiO_2 ratio	Dieletric	
			Constant	Loss
1	PBz-BN/TiO_2	0	3.2	0.94
2		1	3.1	0.93
3		3	3.0	0.87
4		5	2.9	0.78

Conclusion

In this study, a novel benzoxazine monomer (Bzo-BN) containing benzonitrile moiety was synthesized using a simple Mannich condensation reaction. Titania particles (with varying contents) were directly mixed with the Bzo monomer and thermally cured undergoing self-polymerization to produce Pbz/TiO_2 composites. The curing behavior of the Bzo monomer and their hybrids with TiO2 has been much accelerated by the presence of benzonitrile group. A sharp increase in the contact angle for the composite Pbz-BN/T5 (146°) was observed even with a very less amount of titania loading (~ 5 wt%). In spite of this, a drastic improvement in thermal i.e., T5 = 378 ℃; T10 = 403 ℃, mechanical i.e., E' = 3.26 GPa and dielectric i.e., ' = 2.9 was obtained for Pbz-BN/T5. These improvements are due to the difference in surface energies between Pbz and inorganic fillers that generated surfaces with various roughness an caused important ameliorations in the thermo-mechanic and dielectric properties of the neat Pbz resin. This type of conventional processing enables the use of low-cost fabrication processes and provides flexibility for designing superhydrophobic surfaces that have enough potential to be utilized in a wide range of practical applications.

References

1. C.H. Lu, Y.C. Su, C.F. Wang, C.F. Huang, Y.C. Sheen, F.C. Chang, Thermal properties and surface energy characteristics of interpenetrating polyacrylate and polybenzoxazine networks. Polymer **49**, 4852–4860 (2008)
2. C.F. Wang, Y.C. Su, S.W. Kuo, C.F. Huang, Y.C. Sheen, F.C. Chang, Low-surface-free-energy materials based on polybenzoxazines. Angew Chem. Int. Ed. **45**, 2248–2251 (2006)
3. L. Qu, Z. Xin, Preparation and surface properties of novel low surface free energy fluorinated silane-functional polybenzoxazine films. Langmuir **27**, 8365–8370 (2011)
4. Y. Liu, W. Zhang, Y. Chen, S. Zheng, Polybenzoxazine containing polysilsesquioxane: preparation and thermal properties. J. Appl. Polym. Sci. **99**, 927–936 (2006)
5. H. Ishida, D.J. Allen, Gelation behavior of near-zero shrinkage polybenzoxazines. J. Appl. Polym. Sci. **79**, 406–417 (2001)
6. S. Wang, L. Feng, H. Liu, T. Sun, X. Zhang, L. Jiang, D. Zhu, Manipulation of surface wettability between superhydrophobicity and superhydrophilicity on copper films. Chem. Phys. Chem. **6**, 1475–1478 (2005)
7. C. Ao, R. Hu, J. Zhao, X. Zhang, Q. Li, T. Xia, W. Zhang, C. Lu, Reusable, salt-tolerant and superhydrophilic cellulose hydrogelcoated mesh for efficient gravity-driven oil/water separation. Chem. Eng. J. **338**, 271–277 (2018)
8. T. He, H. Zhao, Y. Liu, C. Zhao, L. Wang, H. Wang, Y. Zhao, H. Wang, Facile fabrication of superhydrophobic Titanium dioxide-composited cotton fabrics to realize oil-water separation with efficiently photocatalytic degradation for water-soluble pollutants. Colloids Surf. A **585**, 124080 (2020)
9. T. Agag, T. Takeichi, Synthesis and characterization of novel benzoxazine monomers containing allyl groups and their high performance thermosets. Macromolecules **36**, 6010–6017 (2003)
10. B.K. Tudu, A. Kumar, Robust and durable superhydrophobic steel and copper meshes for separation of oil-water emulsions. Prog Org. Coat. **133**, 316–324 (2019)
11. C. Yu, S. Sasic, K. Liu, S. Salameh, R.H.A. Ras, J.R. van Ommen, Nature-inspired self-cleaning surfaces: mechanisms, modelling, and manufacturing. Chem. Eng. Res. Des. **155**, 48–65 (2020)
12. J. Shi, L. Zhang, P. Xiao, Y. Huang, P. Chen, X. Wang, J. Gu, J. Zhang, T. Chen, Biodegradable PLA nonwoven fabric with controllable wettability for efficient water purification and photocatalysis degradation. ACS Sustainable Chem. Eng. **6**, 2445–2452 (2018)
13. T. Agag, T. Takeichi, Synthesis and properties of silica modified polybenzoxazine. Mater Sci. Forum **449**, 1157–1160 (2004)
14. T. Agag, T. Takeichi, 'Novel benzoxazine monomers containing p-phenyl propargyl ether: Polymerization of monomers and properties of polybenzoxazines'. Macromolecules **34**, 7257–7263 (2001)
15. T. Agag, T. Takeichi, Synthesis and characterization of benzoxazine resin-SiO_2 hybrids by sol-gel process: The role of benzoxazine-functional silane coupling agent. Polymer **52**, 2757–2763 (2011)

16. H. Ji, R. Zhao, Y. Li, B. Sun, Y. Li, N. Zhang, J. Qiu, X. Li, C. Wang, Robust and durable superhydrophobic electrospun nanofibrous mats via a simple Cu nanocluster immobilization for oil-water contamination. Colloids Surf. A **538**, 173–183 (2018)
17. C. Zhu, J. Shi, S. Xu, M. Ishimori, J. Sui, H. Morikawa, Design and characterization of self-cleaning cotton fabrics exploiting zinc oxide nanoparticle-triggered photocatalytic degradation. Cellulose **24**, 2657–2667 (2017)
18. M. Ghashghaee, M. Fallah, A. Rabiee, Superhydrophobic nanocomposite coatings of poly(methyl methacrylate) and stearic acid grafted CuO nanoparticles with photocatalytic activity. Prog Org. Coat. **136**, 105270 (2019)
19. H. Li, P. Mu, J. Li, Q. Wang, Inverse desert beetle-like ZIF-8/ PAN composite nanofibrous membrane for highly efficient separation of oil-in-water emulsions. J. Mater. Chem. A **9**, 4167 (2021)
20. W. Zhang, X. Lu, Z. Xin, C. Zhou, A self-cleaning polybenzoxazine/TiO_2 surface with superhydrophobicity and superoleophilicity for oil/water separation. Nanoscale **7**, 19476–19483 (2015)
21. C.-X. Wang, X.-F. Zhang, A non-particle and fluorine-free superhydrophobic surface based on one-step electrodeposition of dodecyltrimethoxysilane on mild steel for corrosion protection. Corros. Sci. **163**, 108284 (2020)
22. S. Afzal, W.A. Daoud, S.J. Langford, Photostable self-cleaning cotton by a copper(II) porphyrin/TiO_2 visible-light photocatalytic system. ACS Appl. Mater. Interfaces **5**, 4753–4759 (2013)
23. P. Raturi, K. Yadav, J.P. Singh, ZnO-nanowires-coated smart surface mesh with reversible wettability for efficient on-demand oil/ water separation. ACS Appl. Mater. Interfaces **9**, 6007–6013 (2017)
24. M. Wu, W. Liu, P. Mu, Q. Wang, J. Li, Sacrifice template strategy to the fabrication of a self-cleaning nanofibrous membrane for efficient crude oil-in-water emulsion separation with high flux. ACS Appl. Mater. Interfaces **12**, 53484–53493 (2020)
25. M.C. Tseng, Y.L. Liu, Preparation morphology and ultra-low dielectric constants of benzoxazine-based polymers/polyhedral oligomeric silsesquioxane (POSS) nanocomposites. Polymer **51**, 5567–5575 (2010)
26. P. Thirukumaran, A. Shakila Parveen, S.C. Kim, Functionalized MWCNTs, an efficient reinforcement for the preparation of eugenol based high performance PBz/BMI/CNT nanocomposites exhibiting outstanding thermo-mechanical properties. New. J. Chem<bvertical-align:super;> </bvertical-align:super;> **41**, 6607–6615 (2017)
27. P. Thirukumaran, A.S. Parveen, M. Sarojadevi, Synthesis and copolymerization of fully biobased benzoxazines from renewable resources. ACS Sustainable Chem. Eng. **2**, 2790–2801 (2014)
28. P. Thirukumaran, A. Shakila, S. Muthusamy, Synthesis and characterization of novel bio-based benzoxazines from eugenol. RSC Adv. **4**, 7959–7966 (2014)
29. T. Periyasamy, S.P. Asrafali, S. Muthusamy, New benzoxazines containing polyhedral oligomeric silsesquioxane from eugenol, guaiacol and vanillin. New. J. Chem. **39**, 1691–1702 (2015)

30. M. Raposo, Q. Ferreira. P.A. Ribeiro, Modern research and educational topics in microscopy, Modern Research and Educational Topics in Microscopy, 2007, 758
31. L. Shena, H. Dinga, W. Wanga. Q. Guob, Fabrication of Ketjen black-polybenzoxazine superhydrophobic conductive composite coatings. Appl. Surf. Sci. **268**, 297 (2013)
32. T.H. Kao, J.K. Chen, C.C. Cheng, C.I. Su, F.C. Chang, Low-surface-free-energy polybenzoxazine/polyacrylonitrile fibers for biononfouling membrane. Polym. J. **54**, 258 (2013)
33. J. Liu, X. Lu, C. Xin ZZhou, Synthesis and Surface Properties of Low Surface Free Energy Silane-Functional Polybenzoxazine Films. Langmuir **29**, 411 (2013)
34. M. Wang, C. Chen, J.J. Ma, Xu, Preparation of superhydrophobic cauliflower-like silica nanospheres with tunable water adhesion. J. Mater. Chem. **21**, 6962 (2011)
35. C. Zhoua, X. Lua, Z. Xina, J. Liua, Y. Zhang, Effect of nano MMT and mesoporous MCM-41 on corrosion resistance of poly (propylene carbonate)-based waterborne polyurethane. Prog Org. Coat. **76**, 1178 (2013)
36. C. Zhou, X. Lu, Z. Xin, J. Liu, Y. Zhang, Hydrophobic benzoxazine-cured epoxy coatings for corrosion protection. Prog. Org. Coat. **76**, 1178–1183 (2013)
37. S. Rimdusit, K. Punson, D. Isala, A. Somwangthanaroj, S. Tiptipakorn, Rheological and thermomechanical characterizations of fumed silica-filled polybenzoxazine nanocomposites. Eng. J. **15**, 1–7 (2011)
38. C. Zhou, X. Lu, Z. Xin, J. Liu, Y. Zhang, Polybenzoxazine/SiO_2 nanocomposite coatings for corrosion protection of mild steel. Corros. Sci. **80**, 269–275 (2014)
39. K.S. Santhoshkumar, R. Nair, C.P. 'Textbook of Polybenzoxazines: Chemistry and Properties', 2010, Smithers publications
40. B. Kristina, S. Vitalij, O. Huseyin, S. Peter, S. Andreas, L. Prado, S. Karl, H. Stefan, A.S. Gerold, Novel ceramic-polymer composites synthesized by compaction of polymer encapsulated TiO_2 nanoparticles. Compos. Sci. Technol. **72**, 65–71 (2011)
41. Y.C. Chen, H.C. Lin, Y.D. Lee, The effects of filler content and size on the properties of PTFE/SiO_2 composites. J. Polym. Res. **10**, 247–258 (2003)
42. X.G. Chen, J.D. Guo, B. Zheng, Y.Q. Li, S.Y. Fu, G.H. Hu, Investigation of thermal expansion of PI/SiO_2 composite films by CCD imaging technique. Compos. Sci. Technol. **67**, 3006–3013 (2007)
43. D. Wenjie, S. Jiajia, W. Yixian, X. Riwei, Y. Dingsheng, Preparation and characterization of polybenzoxazine/trisilanol polyhedral oligomeric silsesquioxanes composites. Mater. Des. **31**, 1720–1725 (2010)
44. Y.C. Chen, H.C. Lin, Y.D. Lee, Preparation and properties of silylated PTFE/SiO_2 organic-hybrids via sol-gel process. J. Polym. Sci., Part A: Polym. Chem. **42**, 1789–1807 (2004)
45. C.F. Wang, Y.C. Su, S.W. Kuo, C. Huang, Y. Sheen, F. Chang, Low surface free energy materials based on polybenzoxazines. Angewandte. Chemie. **45**, 2248–2251 (2006)

46. Y.C. Chen, H.C. Lin, Y.D. Lee, The effects of phenyltrimethoxysilane coupling agents on properties of PTFE/Silica composites. J. Polym. Res. **11**, 1–7 (2004)
47. N.N. Ghosh, B. Kiskan, Y. Yagci, Polybenzoxazines-new high performance thermosetting resins: Synthesis and properties. Prog. Polym. Sci. **32**, 1344–1391 (2007)
48. Y. Yagci, B. Kiskan, N.N. Ghosh, Recent advancement on polybenzoxazine a newly developed high performance thermoset. J. Polym. Science: Part A: Polym. Chem. **47**, 5565–5576 (2009)
49. B. Kiskan, B. Gacal, M. Atilla Tasdelen, D. Colak, Y. Yagci, Design and synthesis of thermally curable polymers with benzoxazine functionalities, Macromolecular Symposia, 2006, 245–246, 27–33
50. D.W. van Krevelen, Some basic aspects of flame resistance of polymeric materials. Polymer **16**, 615–620 (1975)
51. Y. Liu, J. Zhang, Z. Li, X. Luo, S. Jing, Run, M., A pair of benzoxazine isomers from o-allylphenol and 4,4’-diaminodiphenyl ether: Synthesis, polymerization behavior, and thermal properties. Polymer **55**, 1688–1697 (2014)
52. J. Liu, X. Lu, Z. Xin, C. Zhou, Synthesis and surface properties of low surface free energy silane-functional polybenzoxazine films. Langmuir **29**, 411–416 (2013)

Figures

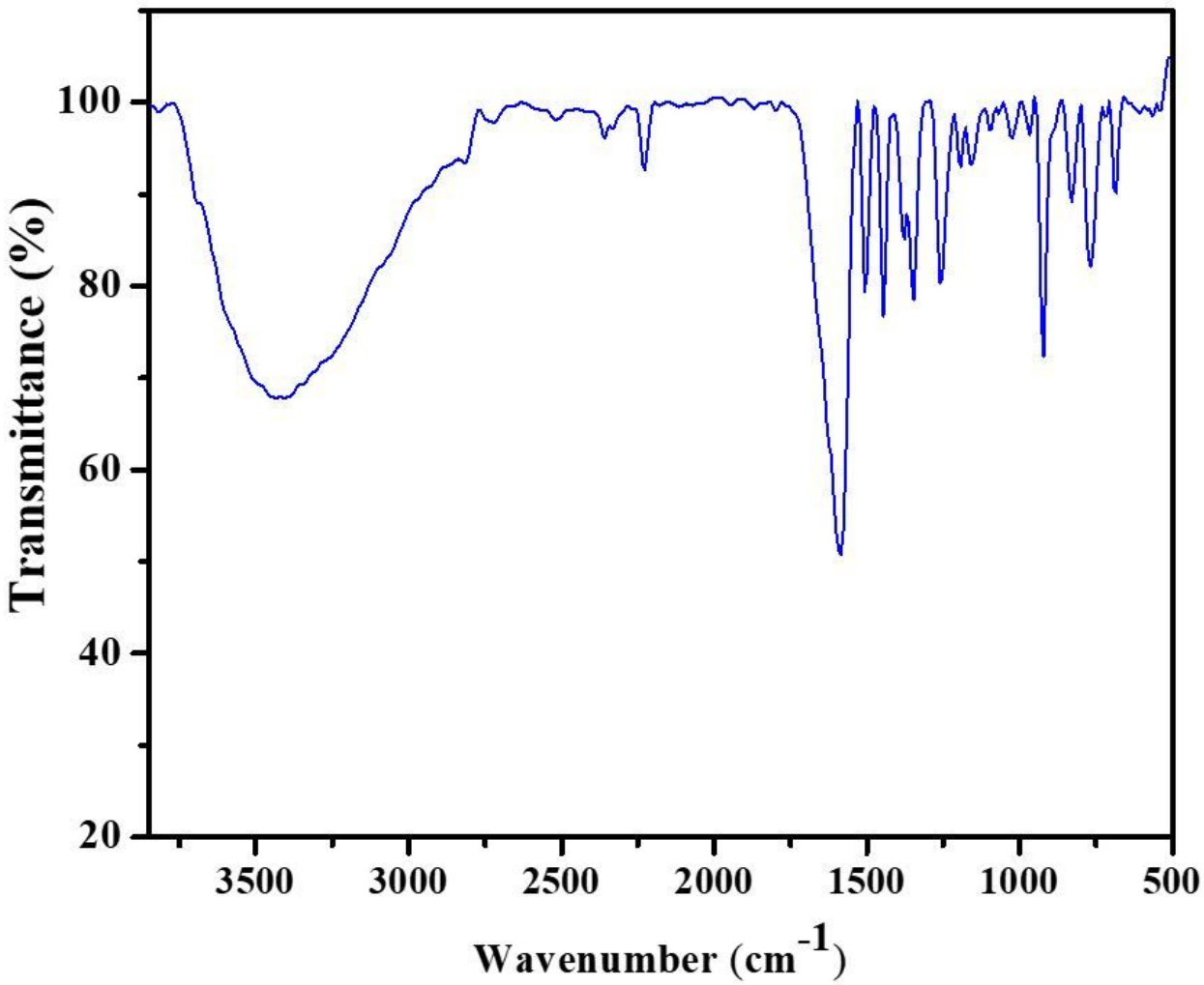

Figure 1

FT-IR spectrum of Bzo-BN

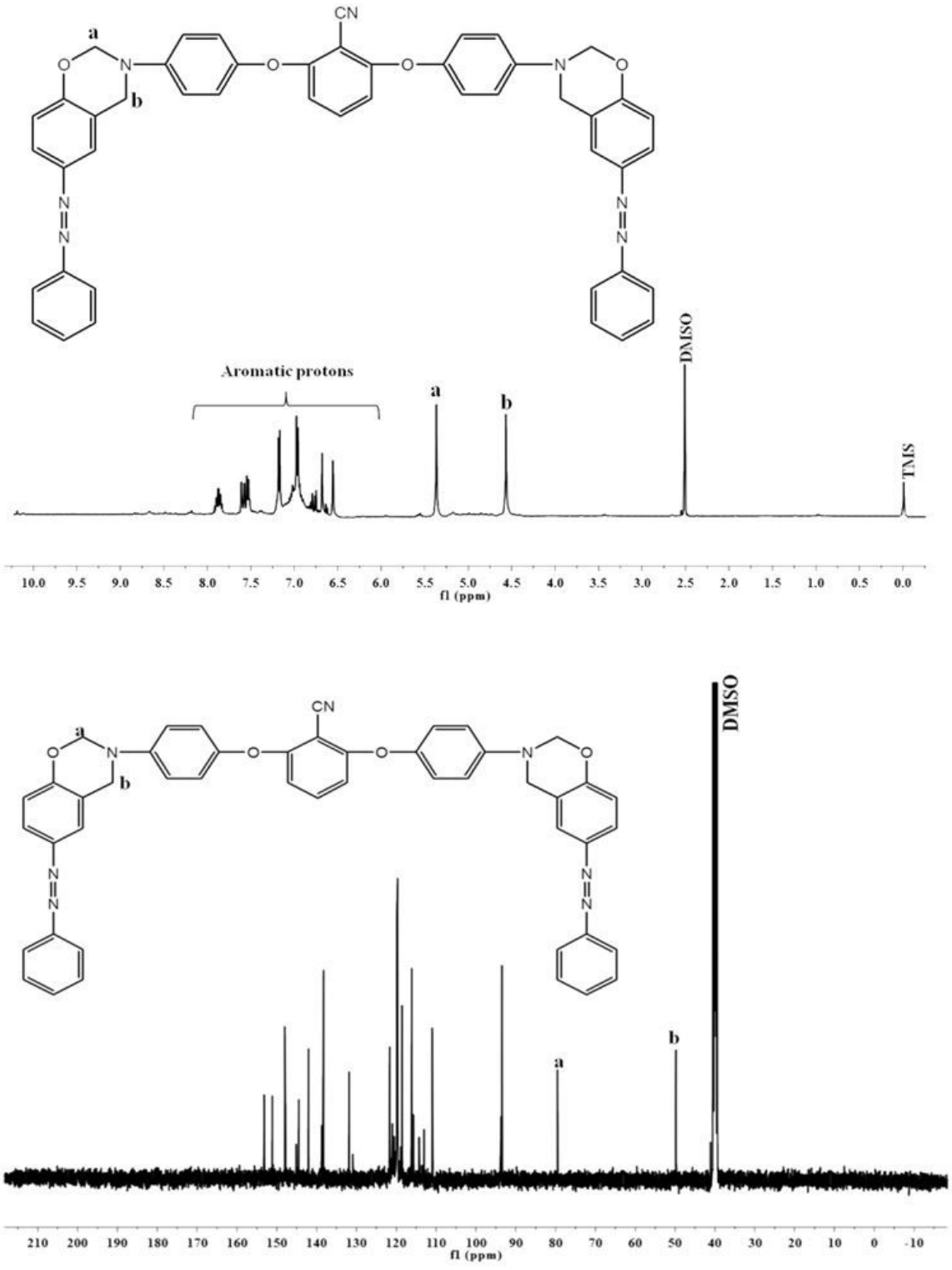

Figure 2

^{1}H- and ^{13}C-NMR spectra of Bzo-BN

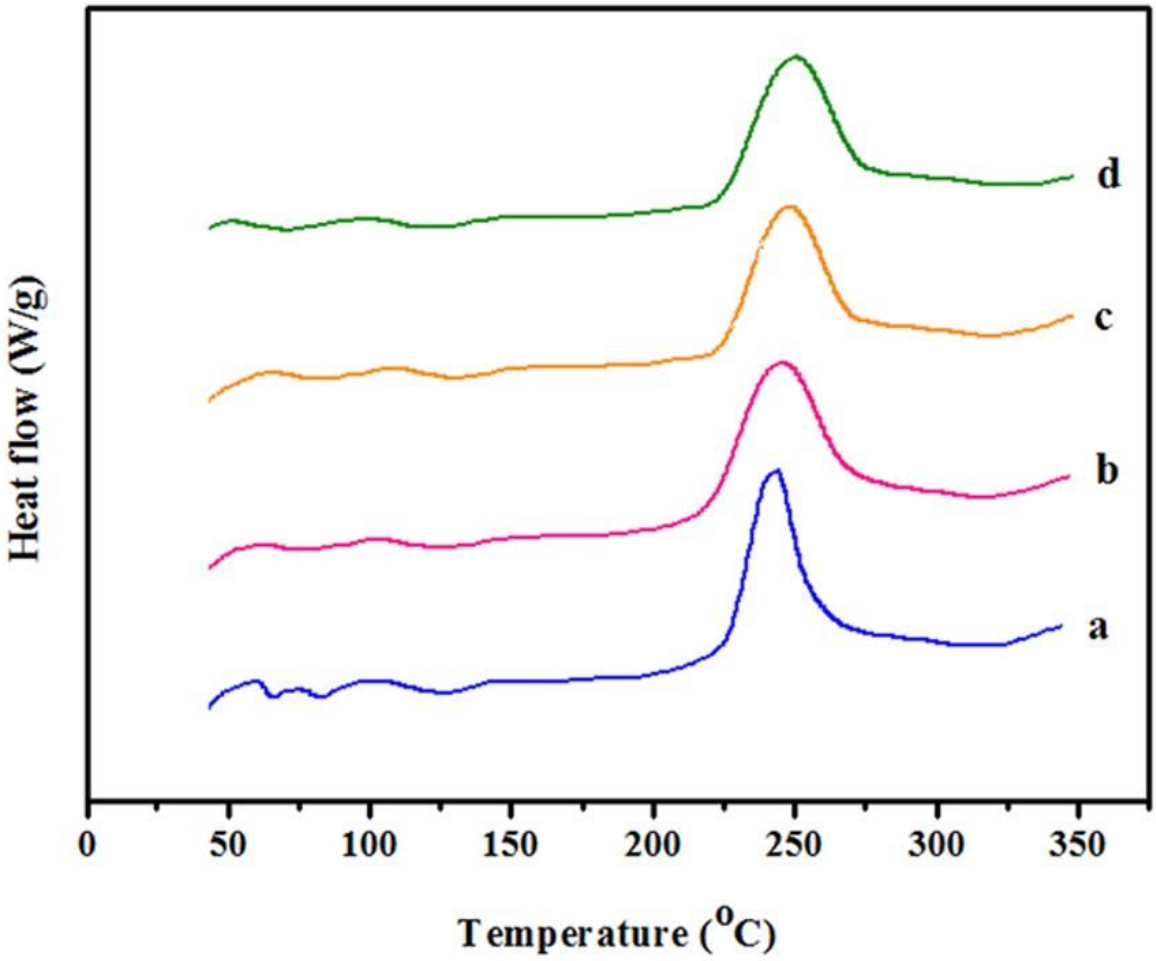

Figure 3

DSC thermograms of (a) Bzo-BN/T0; (b) Bzo-BN/T1; (c) Bzo-BN/T3; (d) Bzo-BN/T5

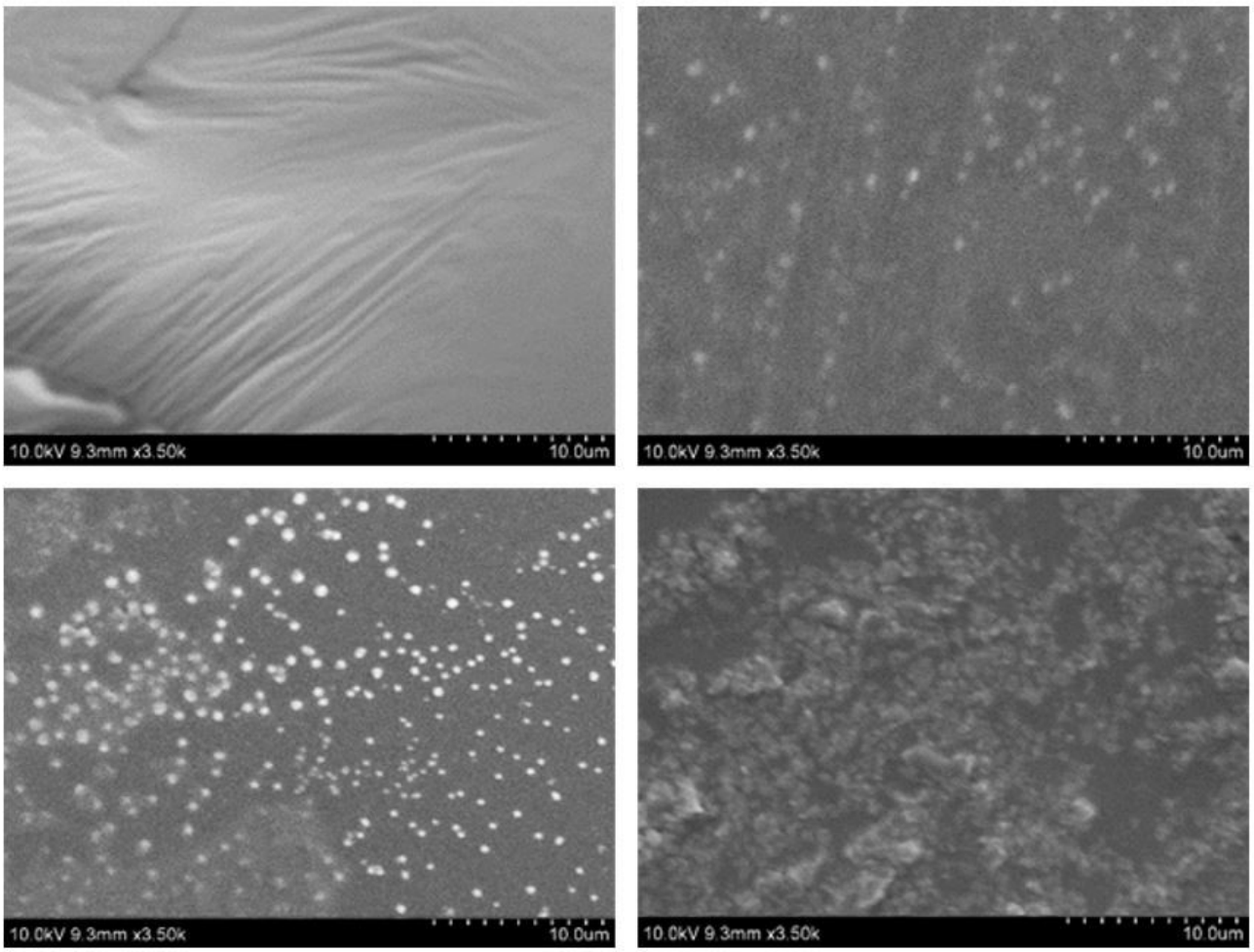

Figure 4

SEM images of (a) Pbz-BN/T0; (b) Pbz-BN/T1; (c) Pbz-BN/T3; (d) Pbz-BN/T5

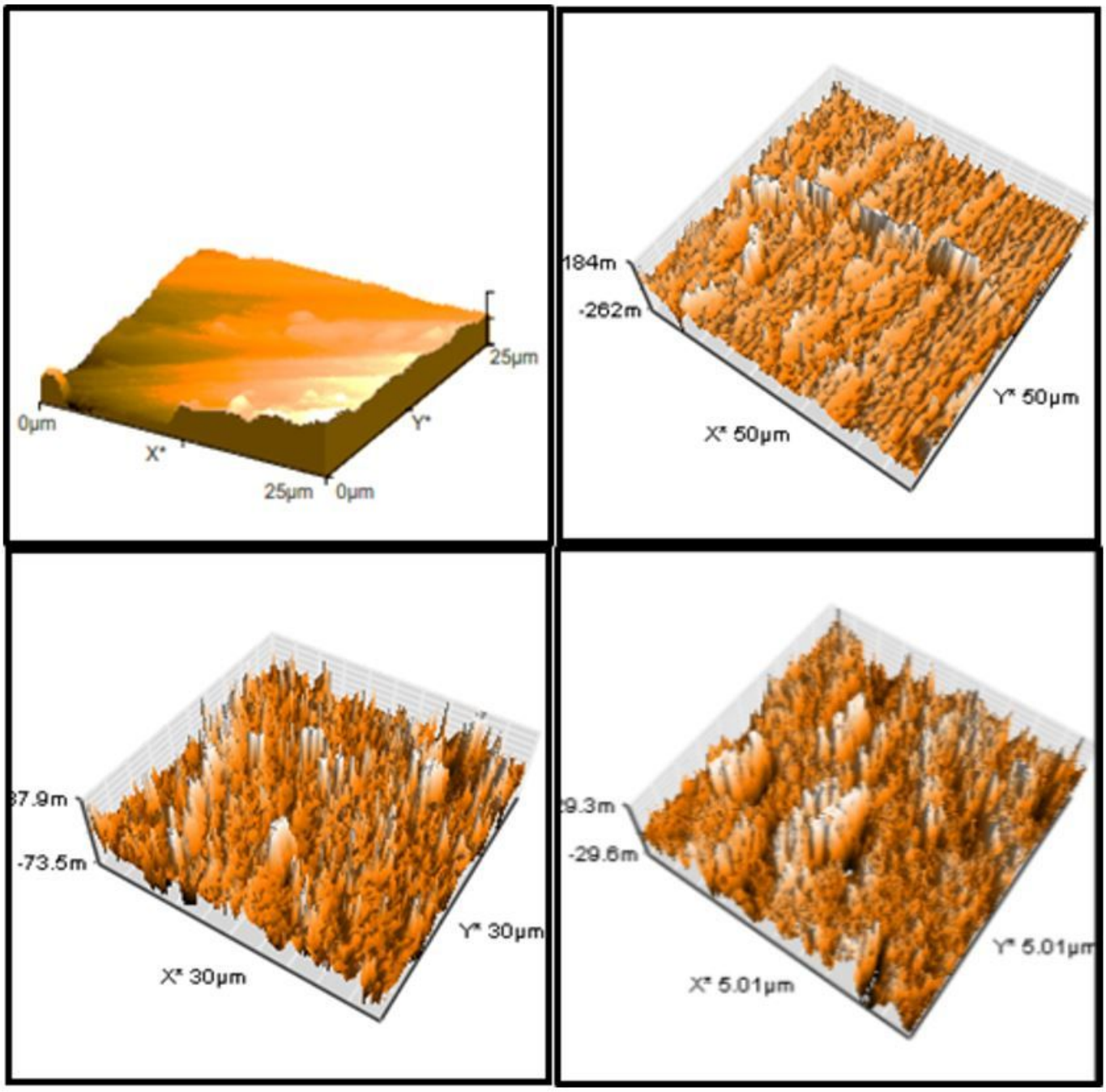

Figure 5

AFM images of (a) Pbz-BN/T0; (b) Pbz-BN/T1; (c) Pbz-BN/T3; (d) Pbz-BN/T5

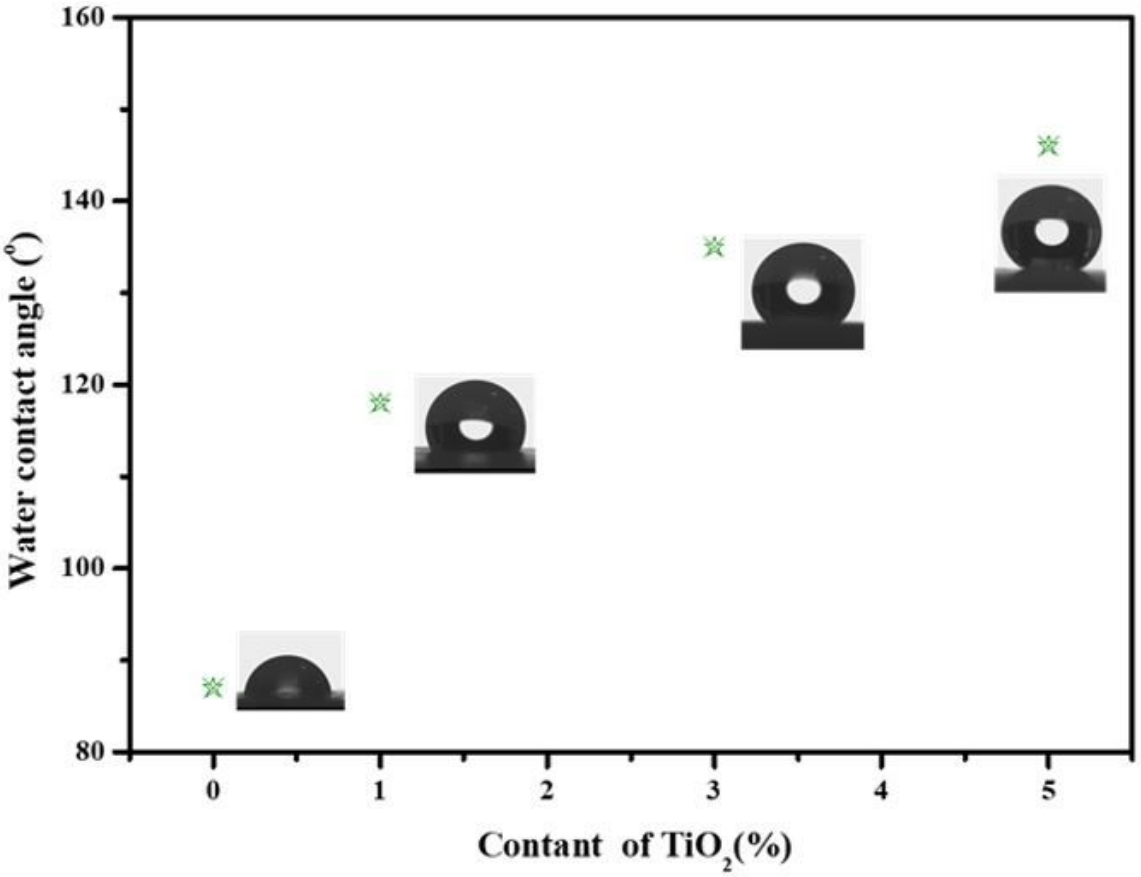

Figure 6

Static WCA of (a) Pbz-BN/T0; (b) Pbz-BN/T1; (c) Pbz-BN/T3; (d) Pbz-BN/T5

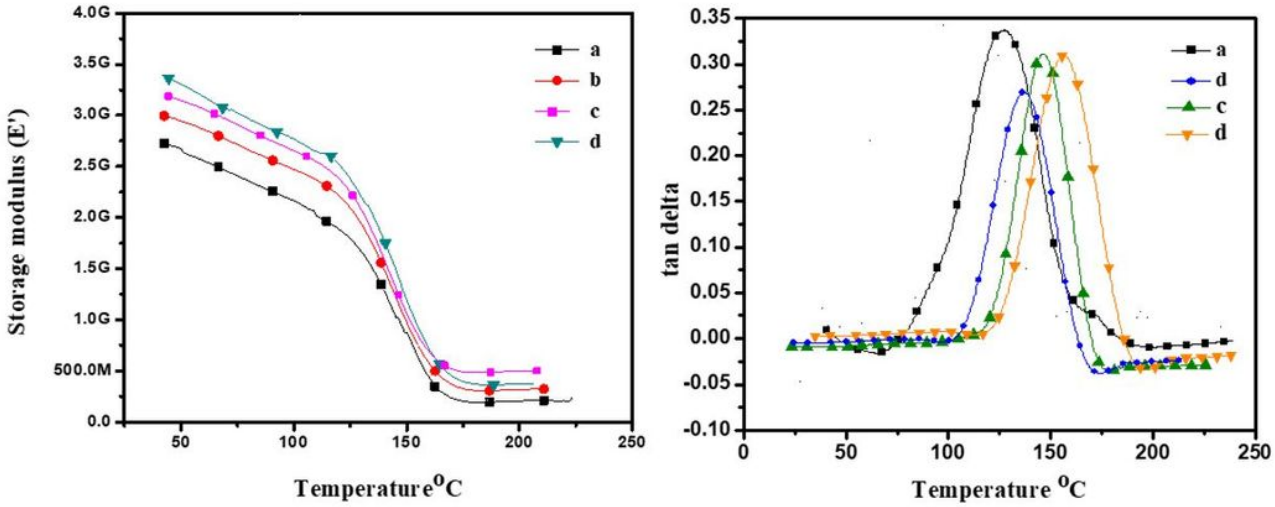

Figure 7

DMA analysis showing storage modulus [7A] and loss modulus [7B] (a) Pbz-BN/T0; (b) Pbz-BN/T1; (c) Pbz-BN/T3; (d) Pbz-BN/T5

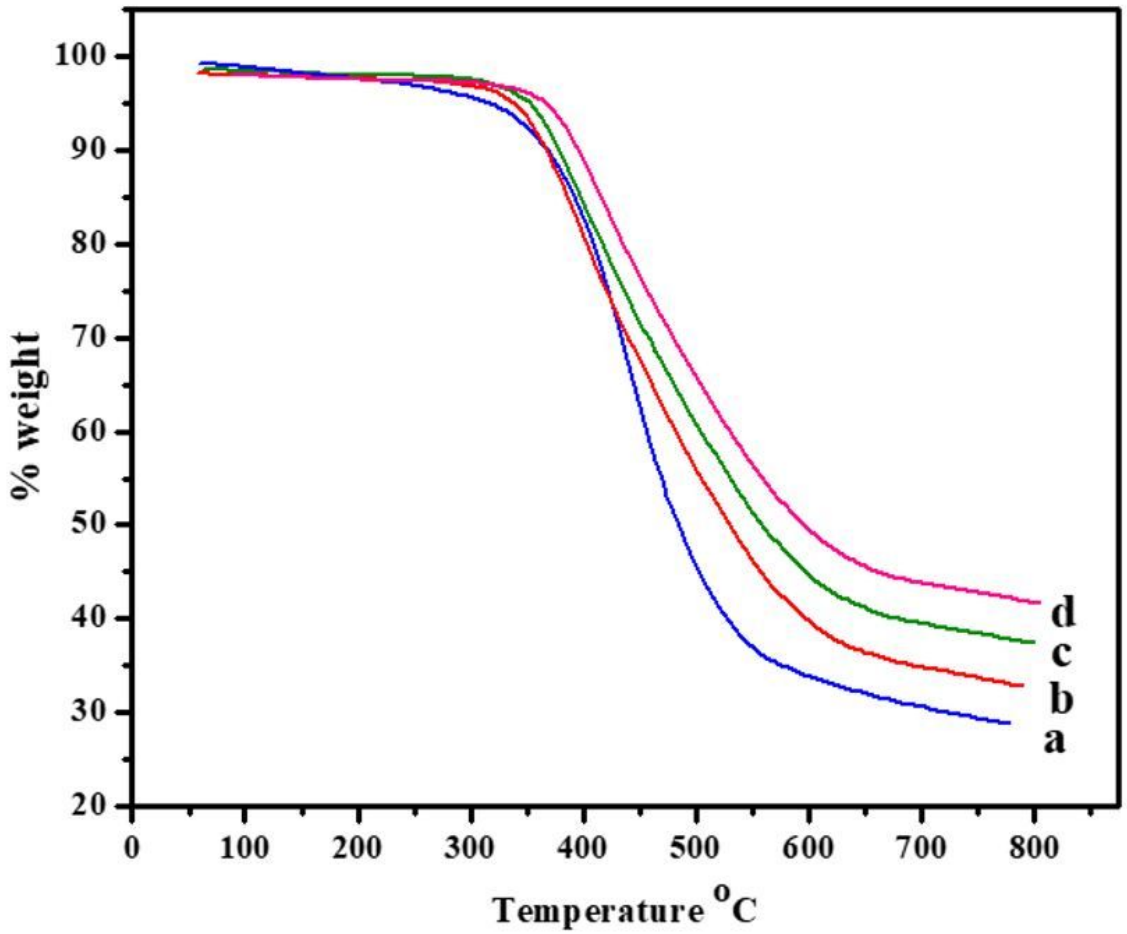

Figure 8

TGA thermograms of (a) Pbz-BN/T0; (b) Pbz-BN/T1; (c) Pbz-BN/T3;

(d) Pbz-BN/T5

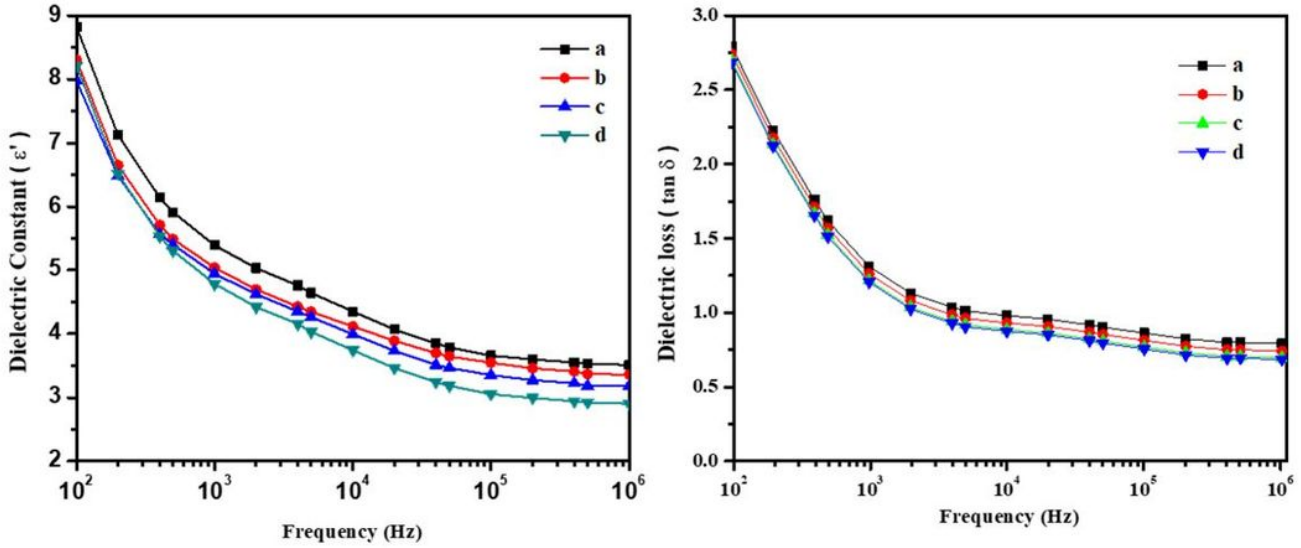

Figure 9

Dielectric constant [9A] and dielectric loss [9B] of (a) Pbz-BN/T0; (b) Pbz-BP/T1; (c) Pbz-BN/T3; (d) Pbz-BN/T5

Supplementary Files

This is a list of supplementary files associated with this preprint. Click to download.

- Supplementarydata.docx